Single-Molecule Spectroscopy

DOI: 10.1002/anie.201006013

Far-Field Nanoscopy with Reversible Chemical Reactions**

*Michael Schwering, Alexander Kiel, Anton Kurz, Konstantinos Lymperopoulos, Arnd Sprödefeld, Roland Krämer, and Dirk-Peter Herten**

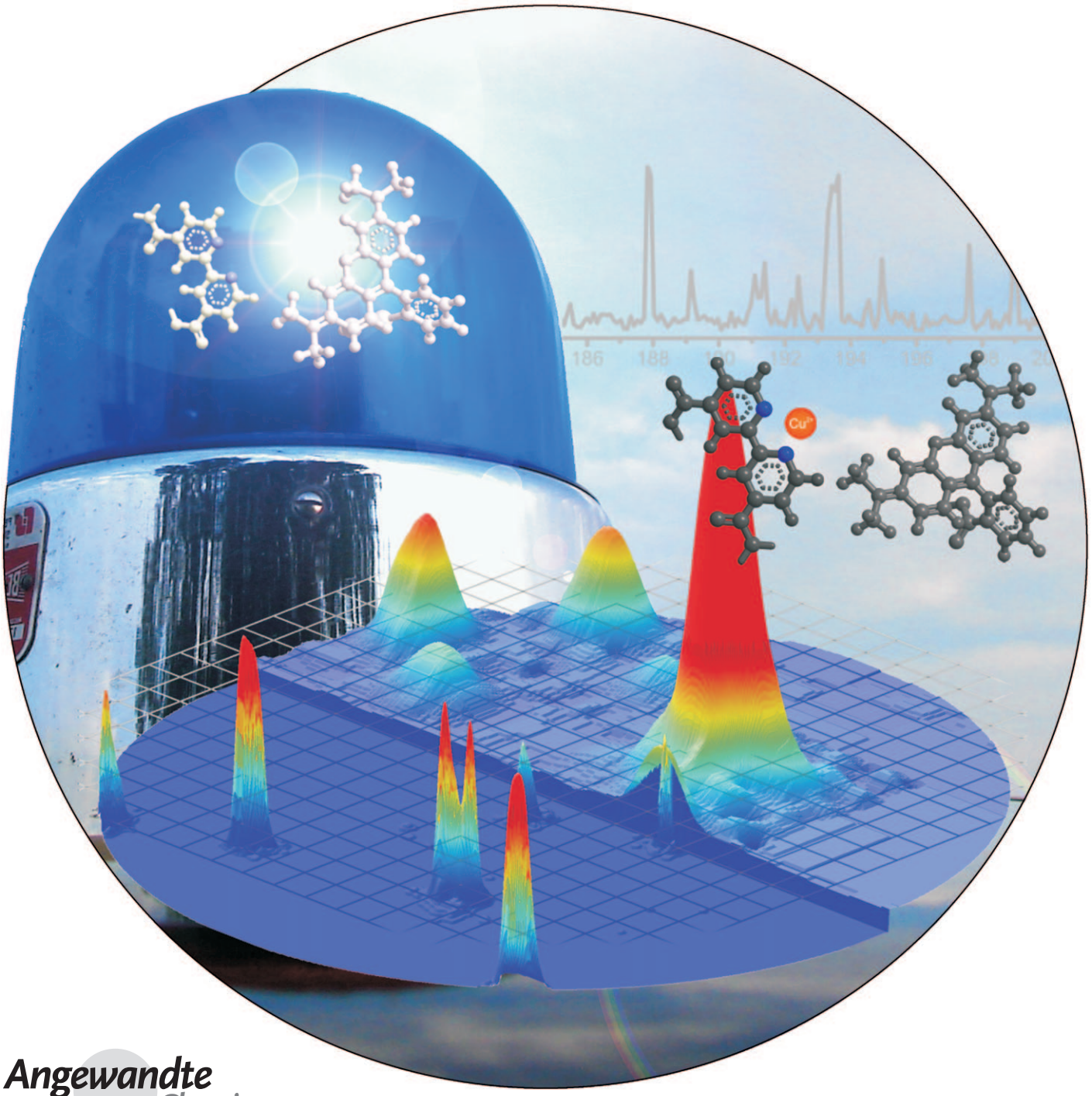

Fluorescence microscopy is a powerful standard tool used to study structures and dynamics in living cells. Its routine application in cell biology has been boosted by the development of genetically encoded fluorescent tags that can be fused to the gene of the target protein and expressed in living cells.[1] However, optical diffraction limits the resolution of far-field microscopy to roughly 200 nm in the lateral plane and around 500 nm along the axis of observation which is 1–2 orders of magnitude larger than many of the macromolecular complexes and clusters of interest.[2]

Recently, several concepts have been experimentally realized that overcome the diffraction barrier and allow optical imaging with an unprecedented resolution in the range of 10–30 nm.[3–6] Most prominent among them are stimulated emission depletion (STED) microscopy and the single-molecule-based stochastic optical reconstruction microscopy (STORM) and photoactivated localization microscopy (PALM).[7–12] These methods separate overlapping point-spread functions of nearby objects in time by light-induced switching of the fluorescent probe between a bright ("on") and a dark ("off") state.

This principle is used in a spatially defined manner in STED microscopy to decrease the size of the point-spread function by a donut-shaped depletion pulse.[8] Images are obtained by raster scanning, and the precision in imaging is determined by the position of the scanning stage, the intensity of the depletion pulse, and the photophysical properties of the dye label.

In contrast, fluorophores and fluorescent proteins in STORM and PALM, respectively, are randomly switched on and off in single-molecule-based methods to image only a small and, in the ideal case, spatially nonoverlapping subpopulation of the fluorescent labels using highly sensitive EMCCD cameras.[9–12] The centers of individual point-spread functions that are now separated in time, that is, in different frames, are then determined with nanometer accuracy. By repeatedly imaging and localizing single fluorophores high-resolution images can be reconstructed.

PALM is based on photoactivation and subsequent photobleaching of fluorescent proteins while in STORM the fluorophores are reversibly cycled between on and off states until photobleaching occurs irreversibly. A crucial point of these methods is that they require an additional excitation line to (re)activate the on state of the fluorescent label during imaging. More recently, STORM was further optimized by controlling the duration of the off state with a reducing and oxidizing system (ROXS), that is, a buffer containing reducing and oxidizing reagents.[13,14] Thereby experimental conditions could further be simplified to a single excitation line suited both for switching of the fluorophores and for imaging.[15] However, the transition from the on to the off state is still light-driven and thus depends on the excitation intensity. Moreover, it has been found that excitation intensity and label density are strongly interrelated.[16] In order to separate individual fluorophores in time at higher label densities the fraction of molecules in the off state has to be increased, usually, by increasing excitation power. Consequently, imaging conditions must be optimized to meet the demands of photoswitching and imaging at the same time as resolution depends on the number of detected photons.[17] Therefore, it would be of general interest to substitute the process of photoswitching with an independent but likewise controllable process. In contrast to STED microscopy, photoswitching in single-molecule-based approaches is stochastic, that is, fluorophores are randomly switched on or off without any spatial or temporal relationship. Therefore, any other stochastic process not triggered by light, like chemical reactions, could theoretically be used for the same purpose if reaction kinetics and quantum yields of the two states are within a suitable range.[18] Very recently, this concept has been realized for localizing catalytically active centers in zeolites and mesoporous silicates using chemical conversions of fluorogenic substrates that either become fluorescent or show a strong change in emission wavelength.[19,20] However, to the best of our knowledge, it has so far not been used in a generally applicable manner to localize biological structures.

Recently, we reported on kinetic measurements for the formation of a copper(II) complex with a bipyridine derivative in thermodynamic equilibrium as a first example of applying single-molecule fluorescence spectroscopy (SMFS) to study homogeneous chemical reactions.[21] In this system, complexation of a Cu^{II} ion is signalled by the distinct quenching of fluorescence intensity of the immobilized probes. In other words, Cu^{II} ions reversibly switch the fluorescent states of the probes between bright (on) and dark (off) states by association and dissociation reactions.

Herein, we present an application of reversible Cu^{II} complexation as a means of stochastic switching for high-resolution microscopy. We name this method CHIRON (CHemically Improved Resolution for Optical Nanoscopy) to underline its chemical nature, but we will use the more general term localization microscopy in the following text. The timescale of switching can be tuned by changing the Cu^{II} concentration.[22] The method is therefore suited for separating individual point-spread functions (PSF) in time, that is, in different frames. Like in STORM, PALM, and related techniques point-spread functions can be localized and used for reconstruction of a high-resolution image.

The probe consists of a double-stranded DNA (22 bp) as a scaffold to bring the chelating ligand 2,2′-bipyridin-4,4′-dicarboxylic acid and the fluorophore tetramethylrhodamine

[*] M. Schwering, Dr. A. Kiel, A. Kurz, Dr. K. Lymperopoulos, Priv.-Doz. Dr. D.-P. Herten
Cellnetworks Cluster & Physikalisch-Chemisches Institut
Universität Heidelberg
Im Neuenheimer Feld 267, 69120 Heidelberg (Germany)
Fax: (+49) 6221-54-51-220
E-mail: dirk-peter.herten@urz.uni-hd.de
Dr. A. Sprödefeld, Prof. Dr. R. Krämer
Anorganisch-Chemisches Institut
Universität Heidelberg
Im Neuenheimer Feld 270, 69120 Heidelberg, (Germany)

[**] We acknowledge financial support from the DFG (EXC 81, SFB 623) and the BMBF (ForSys, VIROQUANT), and we thank Markus Sauer (Universität Würzburg) and Steve Wolter (Universität Bielefeld) for providing software for data analysis.

Supporting information for this article is available on the WWW under http://dx.doi.org/10.1002/anie.201006013.

(TMR) into close proximity as has already been described in previous publications.[22,23] The bipyridine ligand is coupled to the amino-modified 5′-end of one DNA strand while the complementary strand is labeled with TMR at its 3′-end. Additionally, the complementary strand is also 5′-biotinylated for labeling with streptavidin. Both strands were purified by HPLC and hybridized prior to the experiments.

For characterization, probes were immobilized on glass cover slides by streptavidin/biotin binding on surfaces coated with bovine serum albumine (BSA) and doped with biotinylated BSA (≈5%), and the probes were studied by total-internal-reflection fluorescence microscopy (TIRFM; see Figure 1 and the Experimental Section).

Single probes were visualized in TIRF microscopy movies as individual diffraction-limited spots (see the Supporting Information). Individual traces with a time resolution of 100 ms were extracted from movies of surface-immobilized probes taken at different $CuSO_4$ concentrations (Figure 1a–c). In the absence of Cu^{II}, immobilized probes show a constant fluorescence emission until photobleaching occurs (Figure 1a). Only after addition of $CuSO_4$ is the stochastic blinking of individual probes observed on the timescale of seconds (Figure 1b and c); we attribute this to consecutive binding and dissociation of Cu^{II} with the probe.[22] In localization microscopy the off/on ratio has been identified as a crucial parameter for resolution enhancement with dependence on label density.[17] Usually, off/on ratios are controlled by tuning the excitation power. In our approach, the off/on ratio is controlled by changing the $CuSO_4$ concentration. An increase of $CuSO_4$ from 200 nM (Figure 1b) to 2 μM (Figure 1c) leads to significantly shorter on times as a result of an increased number of association events.[19]

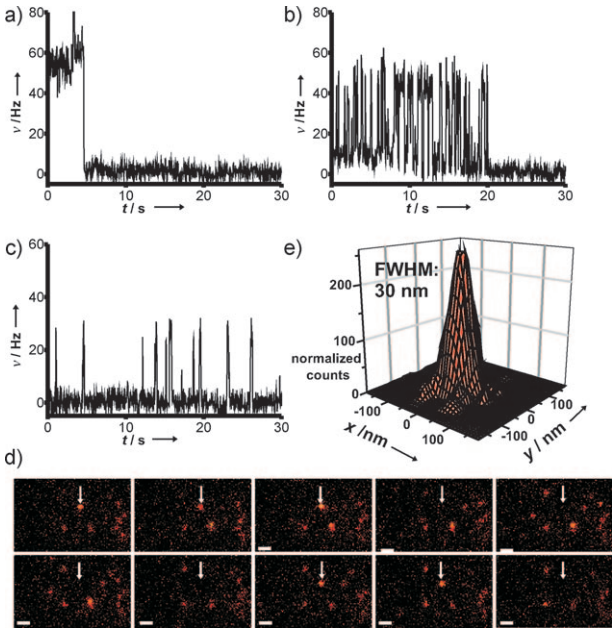

Figure 1. Time-resolved TIRF microscopy (excitation 532 nm, 600 μW; frame rate 30 Hz; 10 ms exposure) of immobilized probes which are quenched upon binding of Cu^{II}. Time-resolved measurements a) in absence of Cu^{II} show constant emission until photobleaching, while at $CuSO_4$ concentrations of b) 200 nM and c) 2 μM discrete random jumps between on and off states occur. d) Frames from a movie at a $CuSO_4$ concentration of 2 μM show that different immobilized probes blink independently of one another and can be resolved and localized individually. The arrow indicates the molecule shown in (c). e) The Gaussian profile yielded from multiple localizations of one spot has a full width at half maximum (FWHM) of 30 nm.

Figure 1d shows individual frames of a movie taken at a frame rate of 30 Hz with an exposure time of 10 ms in the presence of 200 nM $CuSO_4$. The arrow indicates the spot plotted in Figure 1b. It is evident that already at 200 nM $CuSO_4$ individual probes can be resolved in different frames because of discrete blinking typical of single-molecule observations. To test whether resolutions similar to those of published localization microscopy techniques can be achieved, the whole movie (1000 frames) was analyzed using a localization software package.[24] Repeated localization of individual spots using a Gaussian fitting model typically yielded a lateral resolution of approximately 30 nm as compared to the diffraction-limited resolution of roughly 250 nm we measured for our TIRF microscope (Figure 1e). The improvement in lateral resolution is about tenfold and thus comparable to that of other approaches using photoswitching and likewise depends on the total number of frames and the number of photons per spot.[7–12]

Next we tested the applicability of this approach to biological samples by labeling microtubules in fixed mouse fibroblasts with a biotinylated monoclonal bovine α-tubulin antibody (see the Experimental Section). As expected from the results in Figure 1a–c, the quality of the images depends on both the labeling density and the $CuSO_4$ concentration. We tried different concentrations of $CuSO_4$ in the range of 1–40 μM (see the Supporting Information). Too low amounts of $CuSO_4$ lead to overlapping point-spread functions and artifacts in the localization analysis (Figure S1a and b), while the label density and photon yield become too low at high concentrations (Figure S1c and d). The best results with our samples were achieved with 12 μM $CuSO_4$. Figure 2a shows the regular TIRF micrograph of a labeled fibroblast after addition of 12 μM $CuSO_4$. The image is the sum of 8000 frames taken over a period of 400 s (20 Hz) and shows microtubules as blurred features. Individual frames were subjected to localization and reconstruction analysis leading to significant improvement in resolution (Figure 2b). Zoomed-in regions show that individual fibers can be resolved after localization (Figure 2d), while the TIRF micrograph shows mostly blurred features (Figure 2c). The improvement in resolution is also exemplified in Figure 2e which shows the intensity profiles of the TIRF micrograph (red line) and the localization micrograph (green line) taken from the images in Figure 2c and d, respectively, along the blue lines. While the TIRF image displays only a broad bump, two distinct features are nicely resolved in the localization micrograph.

It is important to note that our localization approach is independent of excitation power as fluorescence quenching in the Cu^{II} complex occurs from the excited singlet state (see also Ref. [19]). To unequivocally prove this, kinetic studies were performed with different excitation powers. Measurements of the on/off fluctuations of probes immobilized on glass cover slips were performed at a frame rate of 20 Hz and

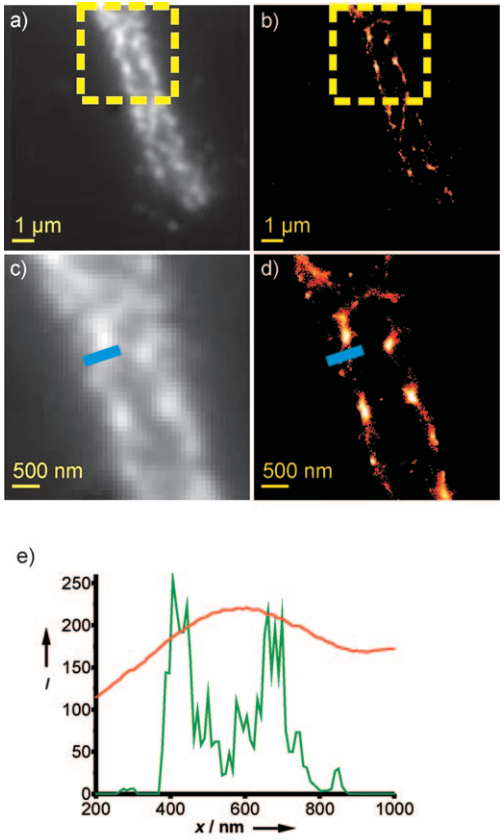

Figure 2. TIRF experiments (excitation 532 nm, 600 μW, frame rate 20 Hz; 12 μM $CuSO_4$) on labeled microtubules of fixed mouse fibroblasts. a) Regular TIRF micrograph integrated over 8000 frames. b) The localized reconstruction of (a) resolves individual microtubules. c,d) Zoomed-in regions of (a) and (b), respectively. e) The intensity profile along the blue line in (c, red) shows a broad feature from the TIRF image. The same profile taken from the localization image (d, green) resolves to distinct features that are not resolved in the TIRF micrograph.

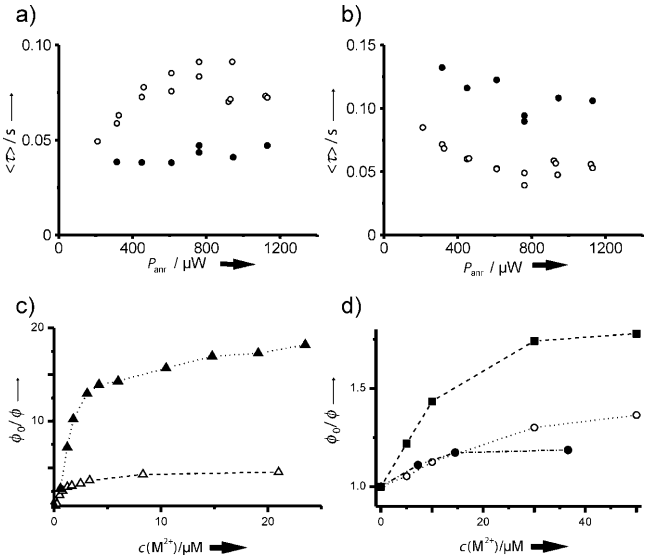

Figure 3. a) The on- and b) off-state durations plotted against excitation power at a $CuSO_4$ concentration of 10 μM (●) and in the absence of Cu^{II} (○). In contrast to the uncomplexed probe, blinking rates are not or only weakly influenced by excitation power. c,d) Stern–Volmer plots showing the inverse relative quantum yield of the probe at varying concentrations of different M^{2+} ions used as quenchers: c) Cu^{II} (▲), Ni^{II} (△); d) Fe^{II} (■), Mn^{II} (○), Co^{II} (●).

an exposure time of 25 ms. Movies were analyzed using the localization software package,[24] and binary (on/off) traces were created from these results for approximately 100 molecules for each experiment. On/off durations were extracted from these traces using a custom MATLAB routine and collected in histograms plotting the relative frequency against on and off duration (see the Supporting Information). These histograms show that on/off duration is not significantly influenced by changes in the excitation power as long as $CuSO_4$ is present in solution. Only in the absence of Cu^{II} does a power dependence become prominent in the on/off durations. The on/off histograms were best fit with an exponential two-component model, and estimated durations as well as the relative amplitude were plotted against excitation power (see the Supporting Information). In the presence of Cu^{II} neither on/off durations nor amplitudes show a systematic trend with changing excitation power. The results are summarized in Figure 3a and b, which show the amplitude-weighted on/off times plotted against excitation power at 0 and 10 μM $CuSO_4$. Obviously, the on duration increases with excitation power when no Cu^{II} is present and levels off or even decreases again at about 800 μW (Figure 3a). The off duration (Figure 3b) first shows a slight decrease with increasing excitation power and also starts to level off at around 800 μW. The reason for these fluctuations is so far unclear and might be as well an artifact of the data analysis by the localization algorithm at low signal-to-noise ratios. More importantly, when Cu^{II} is present, on times remains almost constant with only minor variations. Off times also show a slight shortening with increasing excitation power. However, this is probably related to the rather large variations in the estimated amplitudes. The data in Figure 3a and b as well as in the Supporting Information demonstrate that quenching in the Cu^{II} complex is much less power dependent than that in the free probe. This suggests that associated complexation kinetics dominates the switching process making the presented localization approach unique in the sense that it no longer depends on photoactivation or -deactivation.

We were also interested in testing the ability of other metal ions known to bind to bipyridines, like Ni, Fe, Co, and Mn, as potential quenchers for chemical switching in localization microscopy. Figure 3c and d show Stern–Volmer plots where the inverse relative quantum yield Φ_0/Φ is plotted against concentration $c(M^{2+})$ of the metal ion salt. The increase of Φ_0/Φ with increasing metal ion concentration indicates that all complexes are quenched upon complexation. The strongest quenching can be observed for Cu^{2+} (Figure 3c). Even Ni^{2+} quenches by about a factor of 10 less (Figure 3c). Both curves show saturation at a concentration of roughly 3 μM, indicating specific complexation by the bidentate bipyridine ligand. Other metal ions, like Fe^{2+}, Mn^{2+}, and Co^{2+}, quench even less although saturation and thus complex formation can still be observed (Figure 3d). Additionally,

Mg^{2+} and Ca^{2+} were tested but no noticeable change in fluorescence emission of the probe was observed. Although Cu^{II} seems to be the most suitable quencher with our probe, the probe could be modified by changing the fluorophore and/or the chelating ligand such that even Mg^{2+} or Ca^{2+} could be used to achieve better compatibility with living cells.

In summary, we have experimentally demonstrated the combination of reversible chemical reactions and spectroscopic states, like the Cu^{II} complexation, can be used for single-molecule-based high-resolution microscopy as an alternative to light-driven approaches. In our approach, suitable on/off ratios can be achieved by controlling the Cu^{II} concentration. Thereby, excitation intensity and wavelength become independent of the switching process and can be tuned for optimal imaging. As a positive side effect we also observe that the photostability of the fluorescent dyes is dramatically improved by the addition of $CuSO_4$. The probe itself is quite versatile because ligand, dye label, and metal cation can be varied easily to further finetune different parameters, like on/off ratio, quantum yield, and excitation and emission wavelengths; thus multiplexing is possible. So far, our experiments have been carried out in fixed cells; whether our scheme is suited for live-cell experiments will be addressed in studies in the near future. The probe in its current state may not be perfect for routine application as it employs short oligonucleotides. However, the oligonucleotides are currently only used as a tether and could be replaced by a smaller more compact structure using synthetic chemistry. This will then allow also the introduction of reactive groups for the direct labeling of proteins, like antibodies, to circumvent the biotin–streptavidin tagging and at the same time lead to fewer artifacts of constant emission. Beyond that many fluorophores are commercially available that are susceptible to quenching by different metal ions. It might be worthwhile to explore, for example, the potential of fluorescent Ca^{2+} and Mg^{2+} indicators that can be functionalized for labeling. An advantage of such indicators is that these ions are already present in cells, making the method probably more suited for live-cell applications.

Experimental Section

TIRFM data was acquired on a custom-built TIRFM setup consisting of a Zeiss Axioinvert 200 equipped with a laser emitting at 532 nm (World Star Tech TECGL-30: 532 nm; 30 mW, cw, Toronto, Canada), which was coupled into to the microscope through the back port. Fluorescence was collected by a microscope lens (Olympus, PlanApochromat TIRF 100×, N.A. 1.45, Center Valley, PA, USA) and separated from excitation light by a dichroic mirror and a bandpass filter (z 532/633 and HQ 585/60, AHF Analysentechnik, Tübingen, Germany). Movies were taken with a back-illuminated EMCCD camera (Andor $iXon^{EM}+$ 897, Dublin, Ireland).

For immobilization of probes for TIRFM measurements we used eight-well LabTek chambers (Fisher Scientific GmbH, Schwerte, Germany) which had been cleaned twice with 1% hydrofluoric acid and deionized water. Surface preparation was carried out in 10 mM phosphate-buffered saline (PBS) at room temperature. First, the surface was incubated with a mixture of 5 mg mL^{-1} BSA and biotinylated BSA (20:1) for 30 min. After three rounds of washing with PBS, the surface was incubated with 100 μg mL^{-1} streptavidin for 30 min followed again by another washing step with PBS. Finally, a solution of the DNA probe (0.3 nM) was added and incubated for 30 min. After washing with 10 mM 3-(*N*-morpholino)propanesulfonic acid (MOPS) buffer (pH 7.5) the samples were ready for microscopy.

For the biological tests, mouse fibroblasts (3T3, NIH, DSMZ, Braunschweig, Germany) were cultured overnight in an eight-well cover glass (Nunc/Thermo Fisher Scientific, Langenselbold, Germany) using phenol-red-free media (DMEM, Sigma Aldrich, Taufkirchen, Germany). After rinsing with 10 mM PBS, cells were fixed with 4% paraformaldehyde (PFA) solution in the presence of Triton X-100 for 20 min and then washed three times with PBS for 5 min. Microtubules were then incubated for 1 h with a biotinylated monoclonal bovine α-tubulin antibody (mouse IgG1, monoclonal 236-10501, biotin-XX conjugate, Invitrogen, Darmstadt, Germany) and subsequently washed three times with PBS. Thereafter 100 μg mL^{-1} streptavidin in PBS was added and incubated for 30 min, and unbound streptavidin was removed by washing five times with PBS. Finally, the DNA probe was added (2 μg mL^{-1}) and antibody-tagged cells were incubated for 30 min. Excess DNA probe was removed by washing five times with PBS. After careful removal of liquids MOPS buffer was added for TIRF microscopy experiments.

Received: September 25, 2010
Published online: February 15, 2011

Keywords: chemical switches · fluorescent probes · localization microscopy · resolution limits · single-molecule spectroscopy

[1] R. Y. Tsien, *Angew. Chem.* **2009**, *121*, 5721 – 5736; *Angew. Chem. Int. Ed.* **2009**, *48*, 5612 – 5621.
[2] E. Abbe, *Arch. Mikrosk. Anat. Entwicklungsmech.* **1873**, *9*, 413 – 468.
[3] S. W. Hell, *Science* **2007**, *316*, 1153 – 1158.
[4] B. Huang, *Curr. Opin. Chem. Biol.* **2010**, *14*, 10 – 14.
[5] G. Patterson, M. Davidson, S. Manely, J. Lippincott-Schwartz, *Annu. Rev. Phys. Chem.* **2010**, *61*, 345 – 367.
[6] M. G. Gustafsson, *Proc. Natl. Acad. Sci. USA* **2005**, *102*, 13081 – 13086.
[7] S. W. Hell, J. Wichmann, *Opt. Lett.* **1994**, *19*, 780 – 782.
[8] T. A. Klar, S. Jakobs, S. W. Hell, *Proc. Natl. Acad. Sci. USA* **2000**, *97*, 8206 – 8210.
[9] E. Betzig, G. H. Patterson, H. F. Hess, *Science* **2006**, *313*, 1642 – 1645.
[10] M. J. Rust, M. Bates, X. W. Zhuang, *Nat. Methods* **2006**, *3*, 793 – 795.
[11] S. T. Hess, T. P. K. Girirajan, M. D. Mason, *Biophys. J.* **2006**, *91*, 4258 – 4272.
[12] M. Heilemann, S. van de Linde, M. Schüttpelz, R. Kasper, B. Seefeldt, A. Mukherjee, P. Tinnefeld, M. Sauer, *Angew. Chem.* **2008**, *120*, 6266 – 6271; *Angew. Chem. Int. Ed.* **2008**, *47*, 6172 – 6176.
[13] J. Vogelsang, R. Kasper, C. Steinhauer, B. Person, M. Heilemann, M. Sauer, P. Tinnefeld, *Angew. Chem.* **2008**, *120*, 5536 – 5540; *Angew. Chem. Int. Ed.* **2008**, *47*, 5465 – 5469.
[14] M. Heilemann, S. van de Linde, A. Mukherjee, M. Sauer, *Angew. Chem.* **2009**, *121*, 7036 – 7041; *Angew. Chem. Int. Ed.* **2009**, *48*, 6903 – 6908.
[15] T. Cordes, J. Vogelsang, M. Anaya, C. Spagnuolo, A. Gietl, W. Summerer, A. Herrmann, K. Müllen, P. Tinnefeld, *J. Am. Chem. Soc.* **2010**, *132*, 2404 – 2409.
[16] S. Van de Linde, S. Wolter, M. Heilemann, M. Sauer, *J. Biotechnol.* **2010**, *149*, 260 – 266.
[17] R. E. Thompson, D. R. Larson, W. W. Webb, *Biophys. J.* **2002**, *82*, 2775 – 2783.

[18] J. Vogelsang, C. Steinhauer, C. Forthmann, I. H. Stein, B. Person-Skegro, T. Cordes, P. Tinnefeld, *ChemPhysChem* **2010**, *11*, 2475 – 2490.
[19] M. B. J. Roeffaers, G. De Cremer, J. Libeert, R. Ameloot, P. Dedecker, A. J. Bons, M. Bückins, J. A. Martens, B. F. Sels, D. E. De Vos, J. Hofkens, *Angew. Chem.* **2009**, *121*, 9449 – 9453; *Angew. Chem. Int. Ed.* **2009**, *48*, 9285 – 9289.
[20] G. De Cremer, B. F. Sels, D. E. De Vos, J. Hofkens, M. B. J. Roeffaers, *Chem. Soc. Rev.* **2010**, *39*, 4703 – 4717.
[21] G. De Cremer, M. B. J. Roeffaers, E. Bartholomeeusen, K. Lin, P. Dedecker, P. P. Pescarmona, P. A. Jacobs, D. E. De Vos, J. Hofkens, B. F. Sels, *Angew. Chem.* **2010**, *122*, 920 – 923; *Angew. Chem. Int. Ed.* **2010**, *49*, 908 – 911.
[22] A. Kiel, J. Kovacs, A. Mokhir, R. Krämer, D. P. Herten, *Angew. Chem.* **2007**, *119*, 3427 – 3430; *Angew. Chem. Int. Ed.* **2007**, *46*, 3363 – 3366.
[23] M. Jäger, A. Kiel, D. P. Herten, F. A. Hamprecht, *ChemPhysChem* **2009**, *10*, 2486 – 2495.
[24] The localization software package was provided by S. Wolter (Universität Bielefeld) and M. Sauer (Universität Würzburg). S. Wolter, M. Schüttpelz, M. Tscherepanow, S. van de Linde, M. Heilemann, M. Sauer, *Journal of Microscopy* **2009**, *237*, 12 – 22.

